Virology 415 (2011) 69–82

Contents lists available at ScienceDirect

Virology

journal homepage: www.elsevier.com/locate/yviro

Subcellular location and topology of severe acute respiratory syndrome coronavirus envelope protein

Jose L. Nieto-Torres [a], Marta L. DeDiego [a], Enrique Álvarez [a,1], Jose M. Jiménez-Guardeño [a], Jose A. Regla-Nava [a], Mercedes Llorente [b], Leonor Kremer [b], Shen Shuo [c], Luis Enjuanes [a,*]

[a] Department of Molecular and Cell Biology, Centro Nacional de Biotecnología (CNB-CSIC), Darwin 3, Campus Universidad Autónoma de Madrid, 28049 Madrid, Spain
[b] Protein Tools Unit, Centro Nacional de Biotecnología (CNB-CSIC), Madrid, Spain
[c] Institute of Molecular and Cell Biology, 61 Biopolis Drive, Proteos, Singapore 138673, Singapore

ARTICLE INFO

Article history:
Received 18 February 2011
Returned to author for revision
10 March 2011
Accepted 31 March 2011
Available online 27 April 2011

Keywords:
SARS
Coronavirus
Envelope protein
Antibodies
Location
Ion channel
Topology

ABSTRACT

Severe acute respiratory syndrome (SARS) coronavirus (CoV) envelope (E) protein is a transmembrane protein. Several subcellular locations and topological conformations of E protein have been proposed. To identify the correct ones, polyclonal and monoclonal antibodies specific for the amino or the carboxy terminus of E protein, respectively, were generated. E protein was mainly found in the endoplasmic reticulum-Golgi intermediate compartment (ERGIC) of cells transfected with a plasmid encoding E protein or infected with SARS-CoV. No evidence of E protein presence in the plasma membrane was found by using immunofluorescence, immunoelectron microscopy and cell surface protein labeling. In addition, measurement of plasma membrane voltage gated ion channel activity by whole-cell patch clamp suggested that E protein was not present in the plasma membrane. A topological conformation in which SARS-CoV E protein amino terminus is oriented towards the lumen of intracellular membranes and carboxy terminus faces cell cytoplasm is proposed.

Introduction

The etiologic agent of severe acute respiratory syndrome (SARS) is a coronavirus (CoV), which is the responsible for the most severe human disease produced by a CoV (van der Hoek et al., 2004; Weiss and Navas-Martin, 2005). SARS-CoV emerged in Guangdong province, China, at the end of 2002 and during 2003 rapidly spread to 32 countries causing an epidemic of more than 8000 infected people with a death rate of around 10% (Drosten et al., 2003; Rota et al., 2003). Since then, only a few community-acquired and laboratory-acquired SARS cases have been reported (http://www.who.int/csr/sars/en/). Nevertheless, CoVs similar to SARS-CoV have been found in bats distributed in different regions all over the planet (Chu et al., 2008; Drexler et al., 2010; Muller et al., 2007; Quan et al., 2010), making the reemergence of SARS possible.

SARS-CoV is an enveloped virus with a single-stranded positive-sense 29.7 kb RNA genome, which belongs to *Coronavirinae* subfamily, genus β (Enjuanes et al., 2008) (http://talk.ictvonline.org/media/g/vertebrate-2008/default.aspx). Several proteins are embedded within the SARS-CoV envelope: spike (S), envelope (E), membrane (M), and the group specific proteins 3a, 6, 7a and 7b (Huang et al., 2006, 2007; Schaecher et al., 2007; Shen et al., 2005). Protected by the viral envelope, there is a helicoidal nucleocapsid, formed by the association of the nucleoprotein (N) and the viral genome (gRNA). The CoV infectious cycle begins when the S protein binds the cellular receptor, which in the case of SARS-CoV is the human angiotensin converting enzyme 2 (hACE-2) (Li et al., 2003; Wong et al., 2004), and the virus enters into the cell. Then, the virus nucleocapsid is released into the cytoplasm, and ORFs 1a and 1b are translated directly from the gRNA, generating two large polyproteins, pp1a and pp1ab, which are processed by viral proteinases yielding the replication–transcription complex proteins (Ziebuhr, 2005; Ziebuhr et al., 2000). This complex associates with double membrane vesicles (Gosert et al., 2002; Snijder et al., 2006) and is involved in viral genome replication and in the synthesis of a nested set of subgenomic messenger RNAs (sgmRNAs) through negative polarity intermediaries in both cases (Enjuanes et al., 2006; Masters, 2006; Sawicki and Sawicki, 1990; van der Most and Spaan, 1995; Zuñiga et al., 2010). CoV proteins M, S and E are synthesized and incorporated in the endoplasmic reticulum (ER) membrane, and transported to the pre-Golgi compartment where M protein recruits S protein and binds E protein (de Haan et al., 1999; Lim and Liu, 2001; Nguyen and Hogue, 1997). In parallel, N protein binds gRNA to

* Corresponding author at: Department of Molecular and Cell Biology, Centro Nacional de Biotecnología (CNB-CSIC), Darwin 3, Cantoblanco, 28049 Madrid, Spain.
E-mail address: L.Enjuanes@cnb.csic.es (L. Enjuanes).
[1] Present address: Centro de Biología Molecular Severo Ochoa (CBMSO), UAM-CSIC, Nicolás Cabrera 1, Campus Universidad Autónoma de Madrid, 28049 Madrid, Spain.

0042-6822/$ – see front matter © 2011 Elsevier Inc. All rights reserved.
doi:10.1016/j.virol.2011.03.029

generate the nucleocapsid that is incorporated into virions through the interaction of N and M proteins during an intracellular budding process (Narayanan et al., 2000). Assembled virions accumulate in vesicles that progress through the secretory pathway, and fuse with the plasma membrane to release viruses into the extracellular media (Tooze et al., 1987).

CoV E protein is a small integral membrane protein whose sequence varies between 76 and 109 amino acids (Arbely et al., 2004; Raamsman et al., 2000). Based on primary and secondary structure, the E protein can be divided into a short hydrophilic amino terminal stretch of between 7 and 12 amino acids, a hydrophobic zone of around 25 amino acids with an α-helix secondary structure that constitutes the transmembrane region of the protein, and a carboxy terminal domain, that comprises the majority of the protein (Torres et al., 2007). Nevertheless, a variety of E protein topologies have been described for different CoVs. Mouse hepatitis virus (MHV) and infectious bronchitis virus (IBV) E proteins expose their carboxy terminal region towards the cell cytoplasm, whereas the amino terminal domain is located towards the luminal side of intracellular membranes for IBV or towards the cytoplasm for MHV (Corse and Machamer, 2000; Raamsman et al., 2000). Transmissible gastroenteritis virus (TGEV) E protein adopts a carboxy terminus luminal, amino terminus cytosolic conformation (Godet et al., 1992). In the case of SARS-CoV two alternative topologies have been proposed. In one of them, the transmembrane region forms a helical hairpin, with the amino and carboxy termini oriented towards the cytoplasm (Arbely et al., 2004; Yuan et al., 2006). In the other one, E protein establishes a single-pass transmembrane conformation with the carboxy terminal domain oriented towards the luminal side and the amino terminal domain remaining oriented towards the cytoplasm (Yuan et al., 2006). Therefore, the precise intracellular topology of SARS-CoV E protein is still under debate and needs to be clarified.

Only a small fraction of the pool of CoV E protein generated during infection is incorporated in virions (Maeda et al., 2001; Raamsman et al., 2000), which suggests an important role of E protein within the cell. Apparently, CoV E protein is mainly distributed in intracellular membranes between ER and Golgi compartments (Lim and Liu, 2001; Nal et al., 2005; Raamsman et al., 2000), where it participates in virus assembly, budding and intracellular trafficking through a not fully understood mechanism. In the case of SARS-CoV, it has been shown that E protein is located in the ER or in the Golgi apparatus using cells expressing tagged versions of the protein (Liao et al., 2006; Nal et al., 2005), however, no studies have been performed using infected cells. Recently it has been reported that E protein displays ion channel activity in the plasma membrane when expressed in mammalian cells (Pervushin et al., 2009), which indirectly suggests the presence of SARS-CoV E protein on the cell surface. These data reinforce the need to clearly determine the subcellular location of SARS-CoV E protein in infected cells and specifically, to clarify whether this protein is located at the plasma membrane.

Different requirements of E protein for virus production have been described among different CoVs. TGEV (an α genus CoV) E protein is essential for the maturation and secretion of recombinant infectious viruses (Ortego et al., 2007, 2002). In contrast, a recombinant MHV (β genus CoV) lacking E gene was infectious although it showed lower titers in cell culture than the recombinant wild type virus (Kuo and Masters, 2003). Similarly, in the case of SARS-CoV, the E gene is not essential, although recombinant SARS-CoV lacking the E gene (rSARS-CoV-ΔE) grew from 20- to 200-fold lower than the wild-type virus (rSARS-CoV *wt*) in monkey or human cells, respectively (DeDiego et al., 2007). In addition, SARS-CoV lacking the E gene was attenuated in two animal models (DeDiego et al., 2007, 2008; Netland et al., 2010) indicating that SARS-CoV E gene may be a virulence factor.

Of the CoV E protein activities, the ion channel activity is one of the most remarkable. Several viral proteins with ion channel activity have been described for other RNA viruses, such as M2 from influenza A virus, p7 from hepatitis C virus, Vpu from human immunodeficiency virus (HIV), or 2B from enterovirus (de Jong et al., 2006; Ewart et al., 1996; Pinto et al., 1992; Wozniak et al., 2010). Nevertheless, the relevance of the SARS-CoV E protein ion channel activity and its possible relationship with virus trafficking and assembly is not known. In vitro studies using artificial lipid bilayers showed that HCoV-229E, MHV, SARS-CoV and IBV E proteins behaved as cation-selective ion channels (Torres et al., 2007; Wilson et al., 2006, 2004). A recent report determined that SARS-CoV E protein expressed in mammalian cells, displayed ion channel activity at the plasma membrane as determined by whole-cell patch clamp (Pervushin et al., 2009). Nevertheless, contradictory results have also been reported indicating that SARS-CoV E protein does not behave as an ion channel at the cell surface (Ji et al., 2009).

The clarification of the cellular localization and topology of the SARS-CoV E protein is a crucial issue to understand the activities of E protein. In this article, we report the generation and characterization of monoclonal and polyclonal antibodies specific for the SARS-CoV E protein as essential tools to address E protein subcellular location and topology. The data presented in this study showed that the SARS-CoV E protein essentially accumulated in the endoplasmic reticulum-Golgi intermediate compartment (ERGIC) when expressed both alone or after SARS-CoV infection. No evidence of E protein presence in the plasma membrane was found using immunofluorescence, immunoelectron microscopy or cell surface protein labeling and purification. In addition, whole-cell patch clamp assays revealed decreased current intensity in the plasma membrane of cells expressing E protein, which is not compatible with an E protein mediated voltage gated ion channel at the cell surface. All these data indicated that the E protein would carry out its direct functions from intracellular membranes. By using the specific antibodies generated in this work and selective permeabilization of plasma or intracellular membranes, we propose a topological conformation for SARS-CoV E protein in which this protein spans intracellular membranes only once, with the E protein amino terminus oriented towards the lumen of intracellular membranes and the E protein carboxy terminus exposed towards the cytoplasm.

Results

Generation and characterization of antibodies specific for SARS-CoV E protein

To determine the cellular localization and topology of SARS-CoV E protein, five independently derived hybridomas producing mAbs specific for SARS-CoV E protein were generated. SARS-CoV E protein is mainly hydrophobic and poorly immunogenic (Fig. 1A). Nevertheless, in silico analysis of the E protein amino acid sequence revealed the presence of two regions located in the amino (Ent) and carboxy terminus (Ect) of the protein with higher probability of inducing an immune response (Fig. 1A). To obtain mAbs recognizing different regions of the protein, three pairs of BALB/c mice were each immunized with affinity chromatography purified full-length SARS-CoV E protein expressed in bacteria, or in a baculovirus system, or with chemically synthesized E protein. Sera from immunized mice were analyzed by ELISA using the three sources of purified E protein, and by immunofluorescence using rSARS-CoV *wt*-infected Vero E6 cells and cells infected with a recombinant virus lacking E gene (rSARS-CoV-ΔE) as a negative control. ELISA and immunofluorescence assays showed that the sera from all immunized animals contained antibodies specific for SARS-CoV E protein (data not shown). However, three of the six mice (one of each pair), which developed the highest titers to E protein died or became sick prior to hybridoma generation. The remaining seropositive mice were boosted with the same antigen used in previous immunizations, and sacrificed to collect their spleens to generate hybridomas. Five hybridomas that produced mAbs positive by ELISA, immunofluorescence and Western

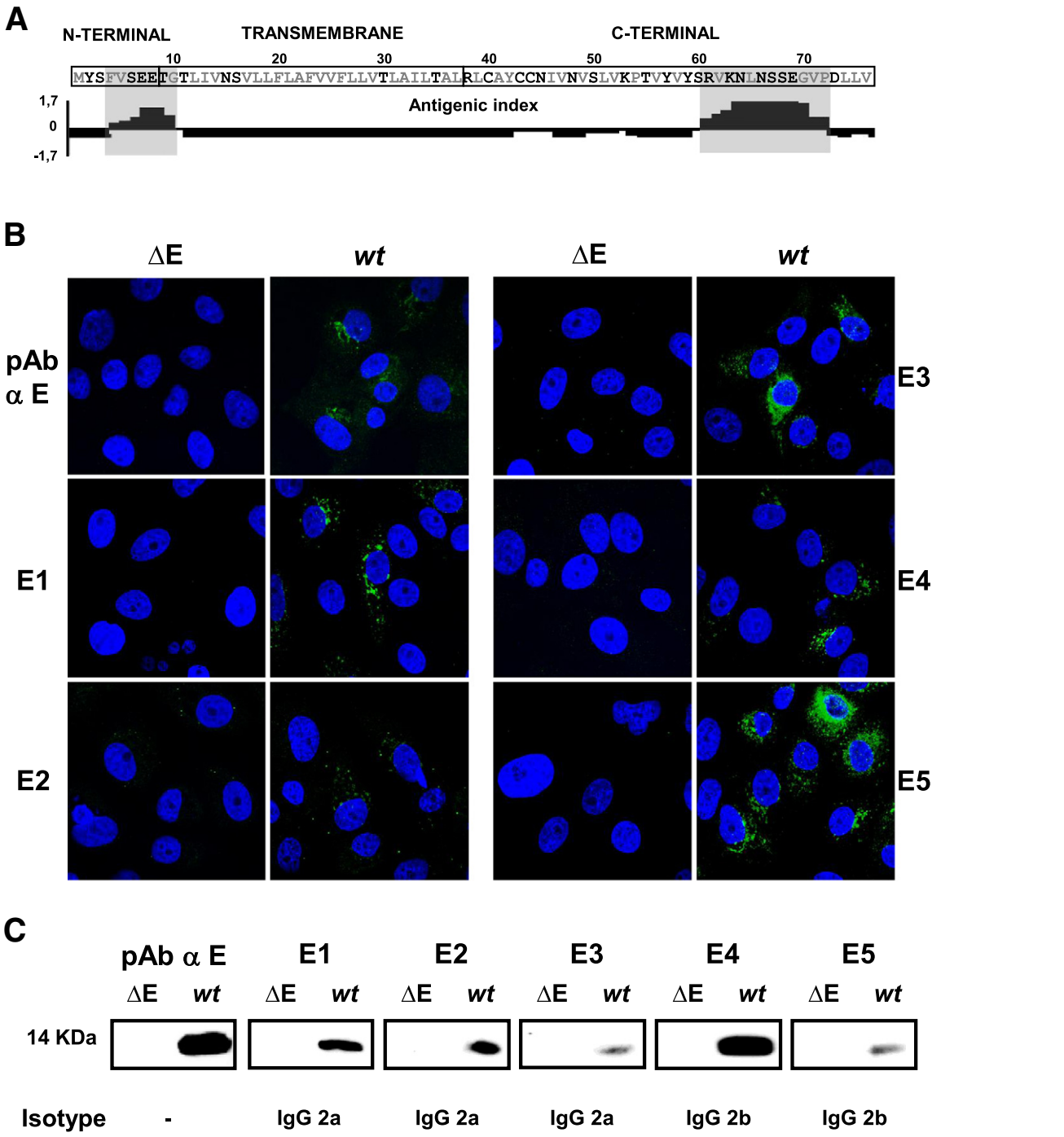

Fig. 1. Characterization of mAbs specific for SARS-CoV E protein. (A) E protein sequence is divided into three domains: the amino terminal (N-terminal), the transmembrane and the carboxy terminal (C-terminal). Gray letters represent hydrophobic amino acids, and black letters indicate hydrophilic amino acids. Jamesson–Wolf antigenic index (DNA-STAR, Lasergene) is shown below the amino acid sequence. Positive values in the graph represent high antigenicity indexes whereas negative values represent low antigenicity indexes. The highest antigenic regions of the protein are shown in gray boxes. (B) Immunofluorescences of SARS-CoV-infected Vero E6 cells. Vero E6 cells were grown on coverslips and infected at an moi of 0.3 with rSARS-CoV *wt* (*wt*) or with rSARS-CoV-ΔE (ΔE) as a control. At 24 hpi cells were fixed with 4% paraformaldehyde, and labeled with E protein specific antibodies (green). Rabbit polyclonal antibody specific for E protein (pAb α E) was used as a control. mAbs are numbered from E1 to E5. (C) Western blot analysis of SARS-CoV-infected Vero E6 cells. Vero E6 cells were infected at an moi of 0.3 with rSARS-CoV *wt* (*wt*) or with rSARS-CoV-ΔE (ΔE) as a control. At 24 hpi cell lysates were collected and probed with mAbs specific for E protein (E1 to E5) or with a polyclonal antibody used as a control (pAb α E). mAbs isotype is indicated bellow Western blot results (C). (For interpretation of the references to color in this figure legend, the reader is referred to the web version of this article.)

blot assays were selected and mAbs were purified by G protein affinity chromatography. All the selected hybridomas were derived from a mouse immunized with the SARS-CoV E protein produced in bacteria. The corresponding purified mAbs (E1, E2, E3, E4 and E5) specifically recognized E protein by immunofluorescence assays on Vero E6 cells infected with rSARS-CoV *wt* but did not bind to the control rSARS-CoV-ΔE infected cells (Fig. 1B). The mAbs showed a staining pattern consistent with a perinuclear distribution of E protein, similar to that observed with a rabbit polyclonal antibody specific for E protein (pAb α E) used as a positive control. Nevertheless, some differences in the staining could be observed. mAb E5 showed the strongest signal and the lowest background in the immunostaining (Fig. 1B). Western blot analysis using protein extracts of rSARS-CoV infected Vero E6 cells showed that all mAbs and the rabbit pAb specific for E protein

recognized a band of approximately 14 kDa, corresponding to E protein. mAb E4 showed the strongest binding by Western blot (Fig. 1C). To analyze the immunoglobulin subclass of each antibody, mAbs were subjected to an ELISA using specific secondary antibodies recognizing the heavy chain of mouse immunoglobulins (IgG1, IgG2a, IgG2b, IgG3 and IgM). Three of the selected mAbs matched to IgG2a isotype and two to IgG2b isotype (Fig. 1C).

To identify the region of E protein recognized by the mAbs, a PEPSCAN epitope mapping was performed. A total of 34 peptides of 10 amino acids covering SARS-CoV E protein full-length sequence were synthesized on a cellulose membrane. Contiguous peptides had eight overlapping amino acids. All mAbs recognized the same two consecutive peptides L_{65}NSSEGVPDL$_{74}$ and S_{67}SEGVPDLLV$_{76}$, representing the end of SARS-CoV Ect domain, although different staining intensities for one or the other peptide were observed with the different mAbs (Fig. 2A). Therefore, these mAbs should recognize the overlapping peptide S_{67}SEGVPDL$_{74}$. The E protein specific polyclonal antibody used as a positive control recognized the same two peptides as the mAbs (L_{65}NSSEGVPDL$_{74}$ and S_{67}SEGVPDLLV$_{76}$) and, in addition, three consecutive peptides, N_{45}IVNVSLVKP$_{54}$, V_{47}NVSLVKPTV$_{56}$ and V_{49}SLVKPTVYV$_{58}$, which are also located in the Ect domain (Fig. 2A). These results indicated that all the antibodies recognized the end of the Ect, suggesting that this domain was the most immunodominant E protein region.

Since all selected mAbs bound the Ect domain, to perform E protein topology studies, polyclonal antibodies specific for Ent domain were generated. To this end, two rabbits were immunized with a peptide corresponding to the first 19 amino acids of the E protein (MYSFVSEETGTLIVNSVLC) coupled to an eight branched polylysine core by a carboxy terminal cysteine. Sera from the two immunized rabbits bound purified E protein produced in bacteria, chemically synthesized E protein, and a peptide containing the Ent domain of the E protein (MYSFVSEETGTL) in an ELISA test (data not shown). Immunofluorescence analysis showed a specific staining of cells transfected with a plasmid expressing E protein (pcDNA-E) or rSARS-CoV *wt*-infected cells but not of cells transfected with the

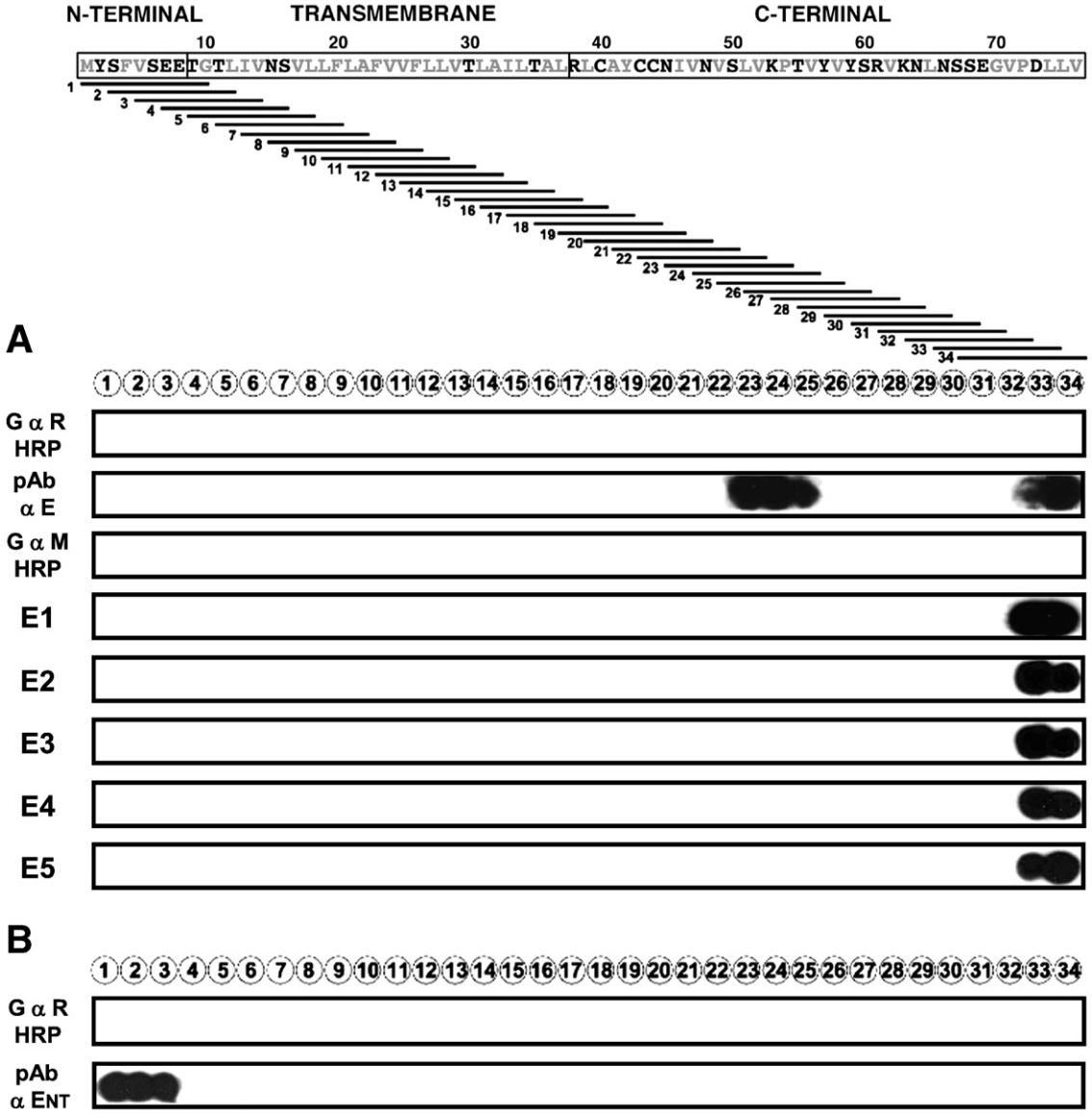

Fig. 2. Epitope mapping of SARS-CoV E protein specific mAbs and pAbs by PEPSCAN. (A) 34 peptides of 10 amino acids each covering the full length SARS-CoV E protein were synthesized on a cellulose membrane. The peptides overlapped contiguous peptides by 8 amino acids. (A) E protein derived peptides were probed by Western blot using a rabbit polyclonal antibody specific for E protein (pAb α E) or using the specific mAbs (E1 to E5). As controls, primary antibodies were omitted and goat secondary antibody coupled to HRP specific for rabbit (G α R HRP) and rabbit secondary antibody coupled to HRP specific for mouse (R α M HRP) were used alone. (B) Epitope mapping of rabbit polyclonal antibody specific for E protein amino terminal domain (pAb α Ent). As a control, a rabbit specific secondary antibody coupled to HRP (G α R HRP) was probed alone.

empty plasmid or infected with the deletion mutant rSARS-CoV-ΔE (data not shown). The serum showing the lowest background in immunofluorescence was analyzed by PEPSCAN epitope mapping. The rabbit antiserum recognized the first three peptides M_1YSFVSEETG$_{10}$, S_3FVSEETGTL$_{12}$ and V_5SEETGTLIV$_{14}$ in which amino terminal domain of SARS-CoV E protein is included. Therefore this pAb most likely recognized the oligopeptide V_5SEETG$_{10}$ (Fig. 2B).

SARS-CoV E protein subcellular localization

The subcellular localization of SARS-CoV E protein was studied in virus-infected cells and in cells transfected with a plasmid encoding the E protein (pcDNA-E). Special focus was devoted to the potential presence of E protein in the plasma membrane, a place where it might display ion channel activity, a remarkable function of this protein. To this end, Vero E6 cells were either infected with rSARS-CoV *wt* or with rSARS-CoV-ΔE as a control, or transfected with the pcDNA-E plasmid or the empty plasmid as a control. Cells were fixed at different hours post infection (hpi) or transfection (hpt), permeabilized, and the subcellular localization of E protein was determined by immunofluorescence, using the E protein specific antibodies previously described and antibodies for the cellular proteins PDI (ER marker), ERGIC53 (ERGIC marker) and cadherin (plasma membrane marker). Confocal microscopy analysis showed similar patterns of E protein distribution in transfected and infected cells at different time points (Fig. 3), suggesting that none of the other viral proteins significantly influenced the subcellular localization of SARS-CoV E protein. At 8 and 16 hpt or hpi E protein mainly colocalized with the ERGIC marker, whereas essentially no colocalization was observed with the ER (in some infected cells a reduced number of colocalization points could be seen), and no colocalization with plasma membrane marker was detected (Fig. 3 and data not shown). Between 24 and 48 hpt or hpi, when the cytopathic effect became evident in infected cells, E protein showed a broader staining pattern in part of the cells (30–40%), which partially overlapped with ERGIC marker, whereas no colocalization was observed with the ER, or with the plasma membrane (Fig. 3 and data not shown). These data showed that SARS-CoV E protein was mainly accumulated within the ERGIC and was not detected at the plasma membrane. To further analyze whether SARS-CoV E protein is present at the plasma membrane, immunofluorescence studies were also performed using non-permeabilized transfected and infected cells, in order to better preserve plasma membrane structure, and antibodies specific for E protein amino and carboxy terminal domains. No specific labeling was detected at the plasma membrane level, reinforcing the previous observations (see below, in SARS-CoV E protein topology section).

To complement the studies on the subcellular localization of SARS-CoV E protein by immunofluorescence, and to further analyze whether E protein was located in the plasma membrane, immunoelectron microscopy analysis was used to determine the presence of SARS-CoV E protein in Vero E6 cells infected with rSARS-CoV *wt* or with rSARS-CoV-ΔE as a control. E protein specific mAb E5 was used in the immunostaining with its corresponding gold-labeled secondary antibody. Gold labeling was analyzed in the plasma membrane and near the viral factories of infected cells. Around 800 gold dots on several micrographs were counted for either rSARS-CoV *wt* or rSARS-CoV-ΔE-infected cells, and gold labeling was referred as gold dots per surface units, considering 12 nm the width of the plasma membrane. Differential gold staining was found in the viral factories of rSARS-CoV *wt*-infected cells as compared with rSARS-CoV-ΔE-infected cells, whereas no specific labeling was found at the plasma membrane as determined by Student's t-test statistical analysis (Fig. 4), what indicated that SARS-CoV E protein was not present at the plasma membrane of rSARS-CoV *wt*-infected cells.

The potential presence of SARS-CoV E protein within the plasma membrane was further studied by biotinylation and purification of cell surface proteins. To this end, Vero E6 cells were infected with either rSARS-CoV *wt* or rSARS-CoV-ΔE as a control. In parallel, cells were transfected with either a pcDNA-E or with the empty plasmid as a control. Plasma membrane proteins were biotin-labeled by incubating cells with Sulfo-NHS-SS-Biotin. This compound is not internalized into cells through the plasma membrane and binds to primary amines of the proteins exposed in cell surface. Cells were lysed and biotinylated proteins were purified by affinity chromatography through a neutravidin Sepharose resin. Cell surface proteins should be biotinylated and captured (B fraction) whereas intracellular proteins should not be biotin-labeled and, therefore, should be present in the chromatography flow through (FT fraction). Complete cell lysates, captured B and flow through FT fractions were analyzed by Western blot using an E protein specific antibody (Fig. 5). In parallel, antibodies recognizing the cytosolic protein β-actin, the endoplasmic reticulum luminal protein GRP78 and the plasma membrane protein cadherin where used as controls of the biotinylation process. Intracellular proteins β-actin and GRP78 were only present in cell lysates and FT fractions but not in B fractions (Fig. 5). In contrast, the plasma membrane protein cadherin was observed in cell lysates, FT fractions and also in B fractions, as expected. E protein was detected in cell lysates and FT fractions of rSARS-CoV wt infected cells and in pcDNA-E transfected cells (Fig. 5), but it was not found in the B fractions, indicating that E protein was not biotinylated, suggesting that this protein was not accumulated at the plasma membrane (Fig. 5).

All together, these data indicated that SARS-CoV E protein is located intracellularly, mainly in the ERGIC, when expressed alone or in a SARS-CoV infection. No evidence of E protein presence in the plasma membrane was found using three complementary assays.

Whole-cell patch clamp assays

To complement and reinforce location studies of E protein in the plasma membrane, ion channel activity measurements were performed by using whole-cell patch clamp. This technique would determine any potential increase in ion currents due to the presence of minor quantities of E protein derived ion channels at the plasma membrane. HEK-293T cells were mock transfected, transfected with an empty plasmid or with a plasmid expressing SARS-CoV E protein (pcDNA-E). At 24 hpt cells were analyzed by the patch-clamp technique in a whole-cell configuration, which allow to measure voltage activated currents corresponding to voltage gated ion channels distributed all over the plasma membrane. Interestingly, control cells without E protein showed high intensity voltage activated currents, whereas cells expressing E protein revealed a significant decrease in current intensities (Fig. 6). These data suggested that E protein was not acting as a voltage gated ion channel present at the plasma membrane, because, that being the case, an increase in voltage activated currents intensity should have been observed in cells expressing E protein as compared with control cells. This finding reinforces our previous conclusion on the absence of E protein within the cell plasma membrane. The observed decrease in current intensity could be due to an indirect effect of E protein on plasma membrane proteins involved in ion transport. In fact we performed E protein pull down assays (Fig. 7), and demonstrated the interaction of SARS-CoV E protein with Na^+/K^+ ATPase alpha 1 subunit and stomatin, that were identified by mass spectrometry with significant Mascot scores (301/80 and 251/70 respectively). Na^+/K^+ ATPase is the main cellular ion pump involved in ion homeostasis control (Kaplan, 2002) and stomatin has been described as an ion channel regulator (Price et al., 2004). These interactions might be responsible for the decrease in the intensity of voltage activated currents in cells expressing E protein.

SARS-CoV E protein topology

It has previously been shown that E protein is an integral transmembrane protein (Liao et al., 2006). To further analyze the topology

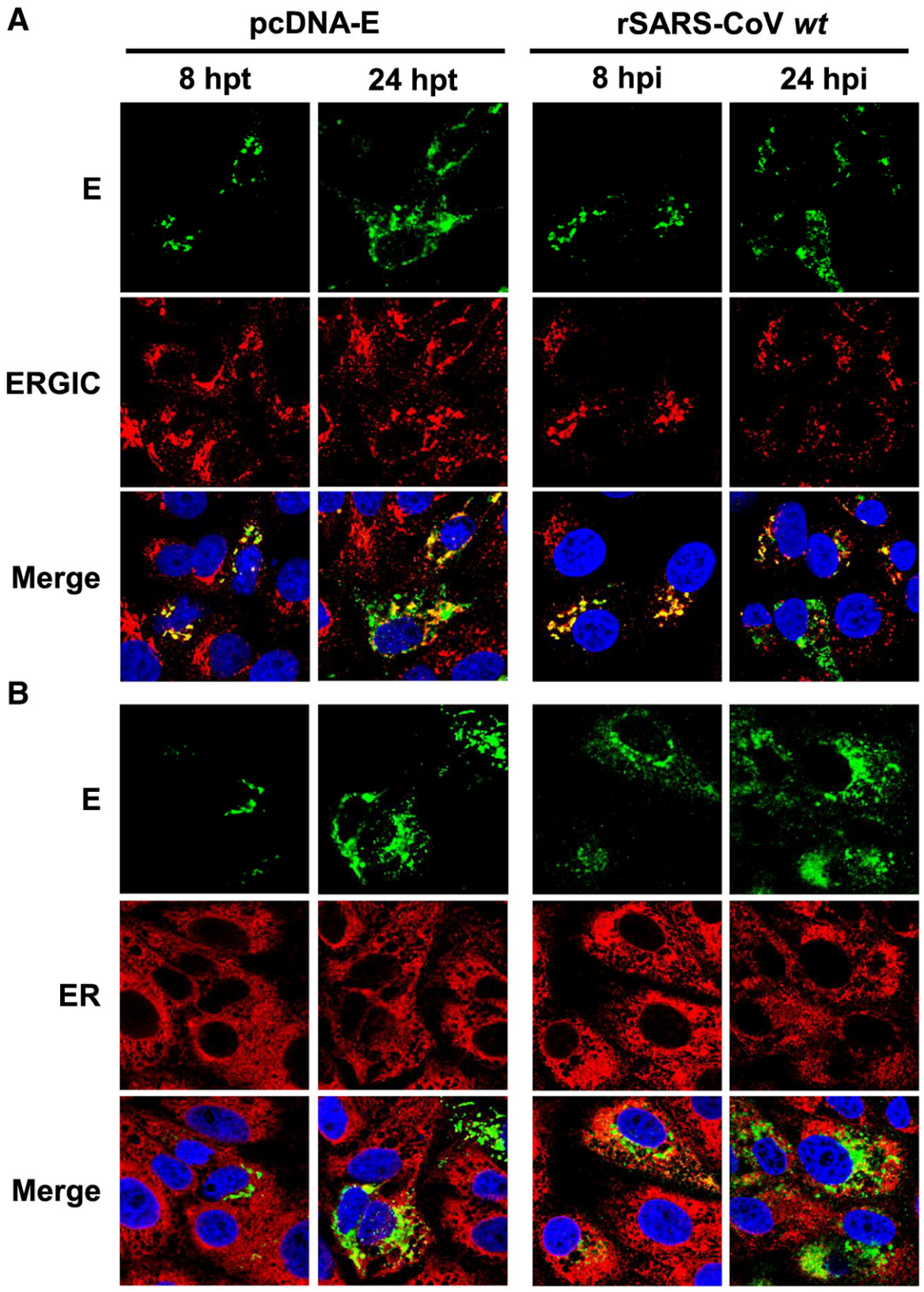

Fig. 3. Subcellular localization of SARS-CoV E protein analysis by immunofluorescence. Vero E6 cells were grown on coverslips and transfected with a plasmid encoding E protein (pcDNA-E) or infected with rSARS-CoV *wt*. Cells were fixed with 4% paraformaldehyde at 8 and 24 h post transfection (hpt) or post infection (hpi). (A) Cells were labeled with E protein (green) or ERGIC53 ERGIC marker (red) specific antibodies. (B) Cells were labeled with E protein (green) or PDI ER marker (red) specific antibodies. (C) E protein was labeled in green and plasma membrane (cadherin) was labeled in red using specific antibodies. Nuclei were stained with DAPI in all cases (blue).

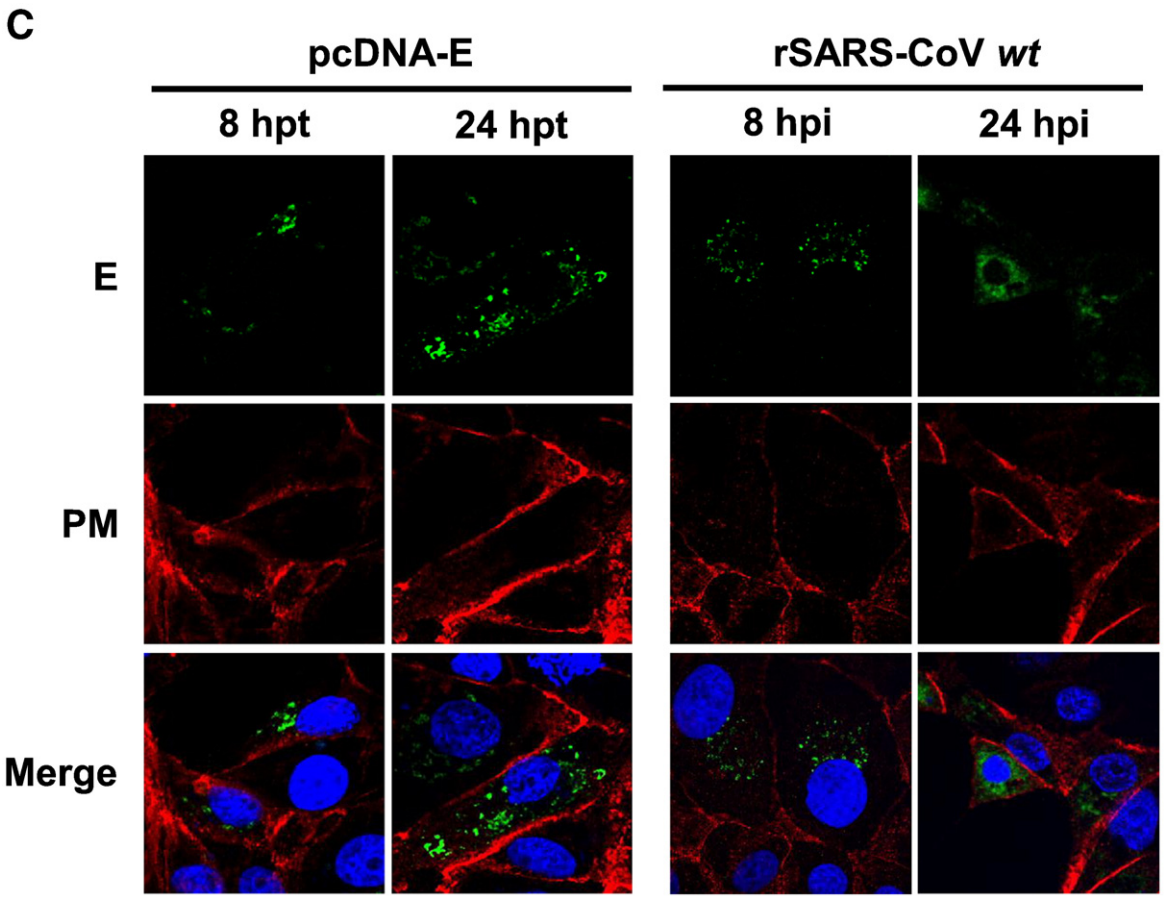

Fig. 3 (*continued*).

of SARS-CoV E protein within cell membranes, antibodies specific for the Ent or Ect domains were used in immunofluorescence assays on detergent permeabilized cells. Vero E6 cells transfected with plasmids expressing E protein or infected with SARS-CoV *wt* were processed either without permeabilization, after permeabilizing their plasma membrane by using digitonin, or after permeabilizing plasma and intracellular membranes by using Triton X-100. An antibody recognizing the cytoplasmic protein β-tubulin, and another one specific for the luminal endoplasmic reticulum protein PDI were used as controls of permeabilization of the plasma membrane or intracellular membranes. The selective permeabilization of the plasma membrane by using digitonin led to the detection of SARS-CoV Ect domain in cells transfected with a plasmid encoding E protein and in SARS-CoV *wt*-infected cells (Fig. 8). Under these conditions, the cytosolic protein β-tubulin was also detected, in contrast to the luminal ER protein PDI that was not accessible, as expected (Fig. 8). Permeabilization of plasma and intracellular membranes with Triton X-100 allowed the detection of SARS-CoV Ect domain, β-tubulin and PDI, as expected (Fig. 8). These experiments were repeated several times with identical results indicating that SARS-CoV Ect domain was exposed towards the cell cytoplasm. In contrast, SARS-CoV Ent domain was only detected when transfected or infected cells were permeabilized with Triton X-100, indicating that this domain must only be exposed towards the luminal side (Fig. 8). Overall, these data indicated that SARS-CoV E protein has a topological conformation spanning the intracellular membranes only once exposing its carboxy terminal domain towards the cell cytoplasm and the amino terminal domain towards the lumen of intracellular membranes.

Discussion

A polyclonal antiserum specific for the SARS-CoV E protein amino terminus, and a set of monoclonal antibodies specific for the SARS-CoV E protein carboxy terminus have been generated. Using these antibodies, SARS-CoV E protein was shown to localize essentially in the ERGIC when expressed alone or in the context of SARS-CoV infection. No evidence for the presence of the SARS-CoV E protein at the plasma membrane has been found by using four complementary approaches. In addition, a topological model for SARS-CoV E protein in which E protein spans intracellular membranes only once and exposes the amino terminal domain towards the lumen of intracellular membranes and the carboxy terminal domain towards the cytoplasm has been proposed.

CoV E protein is involved in virus budding, morphogenesis and intracellular trafficking and possesses ion channel activity (DeDiego et al., 2007; Ortego et al., 2007; Wilson et al., 2006). In previous publications, different authors have proposed alternative cellular locations (ER, Golgi membranes, and plasma membrane) or topologies (spanning membranes once or twice) for SARS-CoV E protein (Liao et al., 2006; Nal et al., 2005; Pervushin et al., 2009; Yuan et al., 2006). To clarify this point, we focused on the subcellular location and topology of SARS-CoV E protein in transfected and infected cells.

In this work, using mAbs specific for the SARS-CoV E protein, and Vero E6 cells, susceptible to SARS-CoV infection, it was shown that E protein was mainly located in the ERGIC at early times (8 and 16 hpi or hpt). Moreover, it was shown that this distribution was extremely similar when E protein was expressed alone from a DNA plasmid or

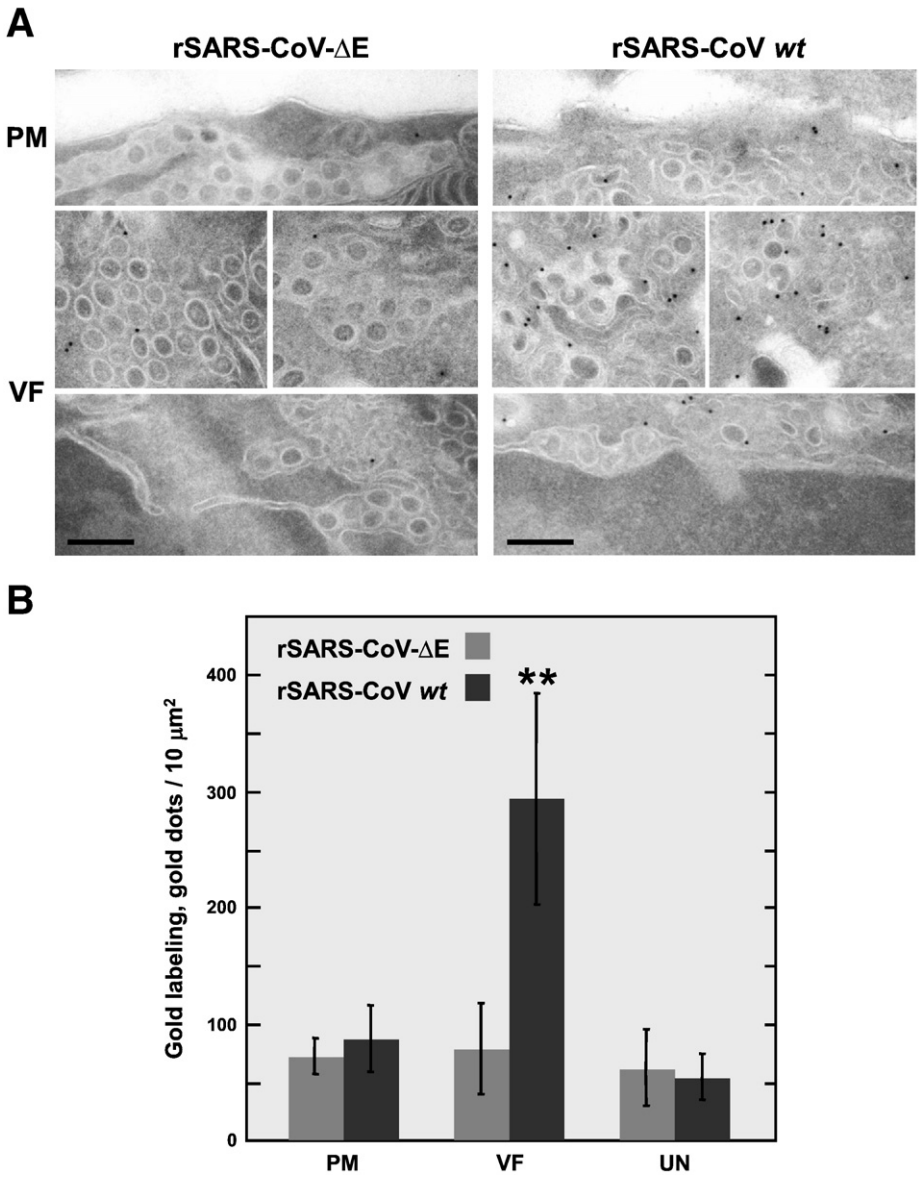

Fig. 4. Analysis of SARS-CoV E protein subcellular localization by immunoelectron microscopy. Vero E6 cells were infected with rSARS-CoV *wt* or rSARS-CoV-ΔE. At 16 hpi cells were fixed with 4% paraformaldehyde and 0.125% glutaraldehyde, scrapped and pelleted. Pellets were processed and sectioned. (A) Ultrathin cryosections were incubated with mAb E5 and an anti-mouse secondary antibody labeled with 10 nm colloidal gold. PM (plasma membrane), VF (Viral factories). Bars 200 nm. (B) Around 800 gold dots were counted in several images of rSARS-CoV-ΔE or rSARS-CoV *wt*-infected cells. Gold labeling is represented as gold dots per surface units (10 μm^2) at the plasma membrane (PM), the viral factories (VF) and at unspecific locations (UN) such as the cell nucleus or mitochondrion, which represent the background displayed by the antibody. Statistically significant data are indicated with two asterisks (Student's t-test p-value$<$0.01).

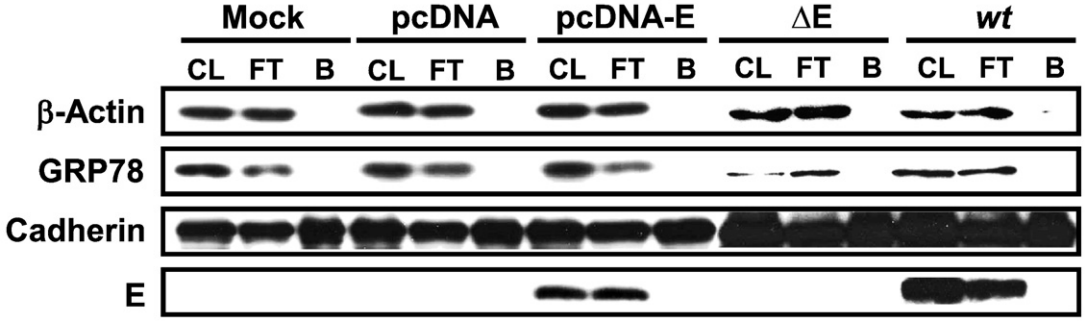

Fig. 5. Analysis of SARS-CoV E protein presence at the plasma membrane by cell surface protein biotinylation and purification assay. Vero E6 cells were either mock transfected, transfected with a plasmid encoding E protein (pcDNA-E) or with an empty plasmid as a control (pcDNA), or infected with rSARS-CoV *wt* (*wt*) or with rSARS-CoV-ΔE (ΔE) as a control. Plasma membrane proteins were biotin labeled and cells were lysed. Cell lysates (CL) were incubated with an avidin resin, and biotinylated cell surface proteins were isolated (B). Non-biotinylated proteins were discarded and eluted in the flow through (FT). CL, FT and B fractions were analyzed by Western blot using antibodies specific for the intracellular proteins β-actin and GRP78, the plasma membrane protein cadherin and SARS-CoV E protein.

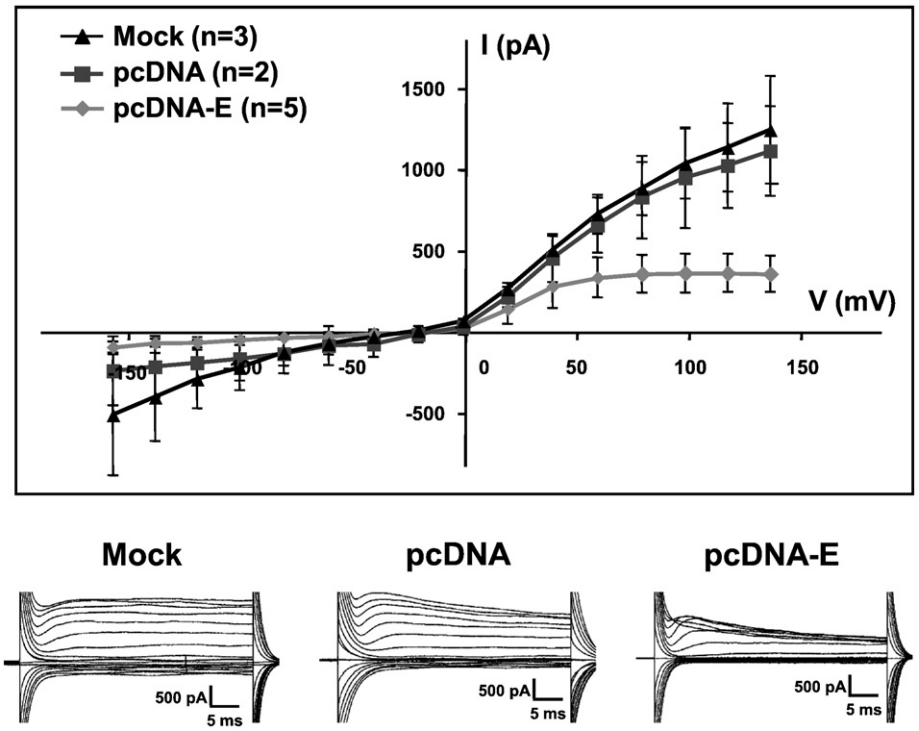

Fig. 6. Whole-cell patch clamp. HEK-293T cells were mock transfected (Mock), transfected with an empty plasmid (pcDNA) or transfected with a plasmid encoding SARS-CoV E protein (pcDNA-E). At 24 hpt cells were voltage clamped, and stepped from −160 mV to +140 mV in 20 mV increments with pulses of 40 ms from a resting potential of −40 mV. Current intensity was plotted against voltage. Currents values were measured at 30 ms, standard deviations are shown. Lower panels show examples of original recordings from each cell type.

after SARS-CoV infection, indicating that other viral proteins did not significantly affected the subcellular location of E protein. At late times, (between 24 and 48 hpi or hpt) 30 to 40% of the cells expressing E protein showed a broader distribution, possibly involving other cell compartments apart from the ERGIC, which might correspond to Golgi modified membranes, similarly to what has been described previously (Liao et al., 2006). The accumulation of E protein at the ER was only found occasionally in infected cells. These data indicated that E protein did not accumulate within this compartment. In contrast to our observations, other reports described that SARS-CoV E protein colocalized with ER and Golgi markers (Liao et al., 2006; Nal et al., 2005). The apparent discrepancies between our results and previous publications, may be explained by the strength of the expression system used, by the use of different cell lines, by performing the studies at different time points and by the use of different tagged versions of E protein. Nevertheless, in the publications by other authors, E protein location was not analyzed in cells infected with SARS-CoV, as done in this paper.

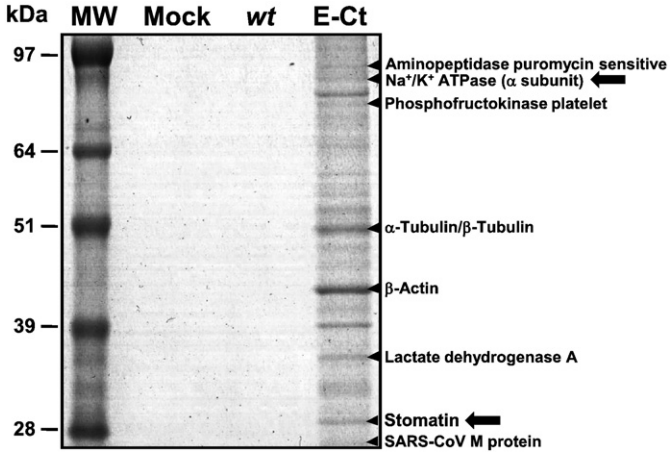

Fig. 7. Identification of proteins interacting with SARS-CoV E protein. Vero E6 cell extracts from mock-infected cells (Mock) or cells infected with rSARS-CoV *wt* or rSARS-CoV-EtagCt (E-tag) were used in a double affinity chromatography. Purified proteins were detected by using Coomassie blue gels. Bands were excised from gels and identified by mass spectrometry. Arrows point Na^+/K^+ ATPase alpha 1 subunit and stomatin protein bands.

It has been reported that E protein displays ion channel activity in the plasma membrane of mammalian cells (Pervushin et al., 2009), which has indirectly suggested that E protein is present on the cell surface. Nevertheless, neither our results shown in this manuscript nor other published work (Nal et al., 2005; Yuan et al., 2006) have provided direct evidence showing the presence of SARS-CoV E protein in the plasma membrane. In fact, special attention was paid in this study to analyze whether SARS-CoV E protein was located in the plasma membrane. Immunofluorescence analysis of cells transfected with a plasmid encoding E protein and SARS-CoV-infected cells, revealed that E protein did not accumulate at the plasma membrane neither at early (8 and 16 hpt or hpi) nor at late time points (24 and 48 hpt or hpi). In addition, immunofluorescence using non-permeabilized cells and antibodies specific for the amino or carboxy terminal domains of E protein did not reveal any specific staining at the cell surface. To reinforce these data immunoelectron microscopy was performed. E protein was identified intracellularly in infected cells, close to viral factories, whereas no significant labeling was observed at the plasma membrane. To further study the possible presence of E protein in the plasma membrane, cell surface proteins were biotinylated and isolated. Protein biotinylation was achieved by using a compound that binds covalently to primary amines, present in lysines side chain and in the protein N-terminal amino acid. If SARS-CoV E protein would be displayed in the plasma membrane, it should expose its amino terminal domain towards the outside of the cell, taking into account our purposed topological conformation. No lysine residues are contained within SARS-CoV E protein amino terminal domain. Nevertheless, the amino group of the

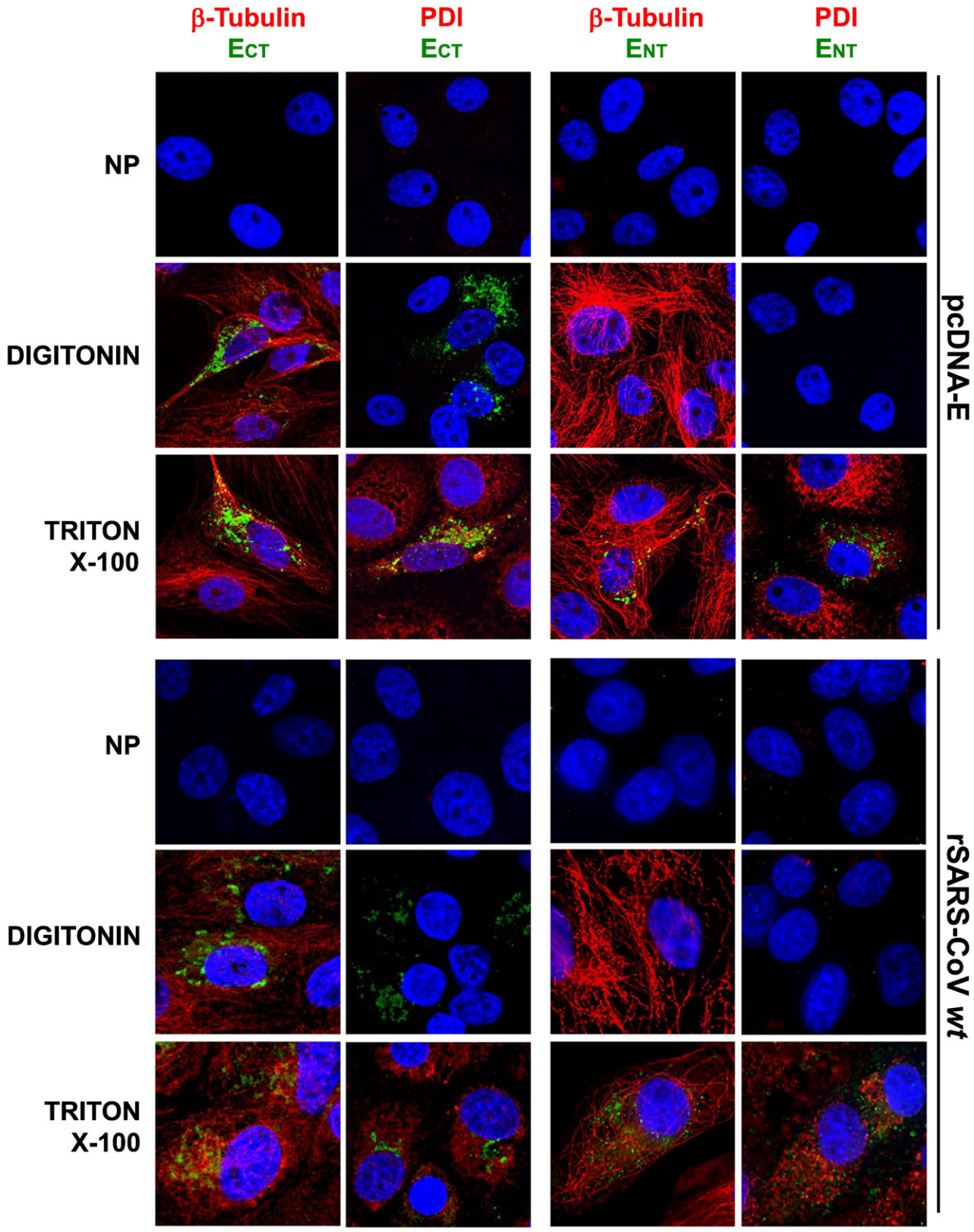

Fig. 8. SARS-CoV E protein topology. Vero E6 cells expressing E protein alone (pcDNA-E) or in an infection context (rSARS-CoV *wt*) were alternatively processed with no permeabilization (NP), selectively permeabilizing plasma membrane by using digitonin or permeabilizing all cell membranes by using Triton X-100. Specific antibodies were used to label the E protein carboxy terminal domain (ECT, green), E protein amino terminal domain (ENT, green), the cytosolic protein β-tubulin (red) and the luminal ER protein PDI (red). Nuclei were stained with DAPI (blue). (For interpretation of the references to color in this figure legend, the reader is referred to the web version of this article.)

N-terminal amino acid would be a potential site of biotinylation. No evidence of biotinylated E protein was detected, indicating that E protein did not accumulate in the plasma membrane.

In order to investigate potential ion channel activity due to the presence of E protein at the cell surface, whole-cell patch clamp assay was performed as a functional approach to alternatively determine

whether SARS-CoV E protein is located at the plasma membrane. If E protein were acting as an ion channel activated by voltage in the plasma membrane, an increase in current intensities displayed by cells expressing E protein, as compared with control cells, would be expected. Interestingly, cells expressing E protein showed a decrease of current intensities as compared with control cells not expressing E protein, suggesting that this protein was not acting as an ion channel at the plasma membrane, and reinforcing the observation that E protein was not physically located within the plasma membrane. The fact that E protein decreased ion currents in the plasma membrane might be explained by an indirect influence of E protein on other cellular proteins involved in ion transport. Recently, in our laboratory, two cellular proteins involved in ion transport: Na^+/K^+ ATPase alpha 1 subunit and stomatin, have been identified as interacting partners of SARS-CoV E protein. Possibly, these interactions could lead to partial relocalization of these proteins and therefore to the observed reduction of ion transport, which may explain decreased voltage activated currents intensity detected by whole-cell patch clamp assays. Importantly, in agreement with our work, it has been shown that E protein does not display ion channel activity in a different experimental system, the plasma membrane of *Xenopus* oocytes (Ji et al., 2009) but decreases the levels and activity of human epithelial sodium channels, affecting ion transport at the plasma membrane level.

Overall, our results from four complementary approaches strongly suggest that SARS-CoV E protein did not accumulate at the plasma membrane during SARS-CoV infection, or when expressed alone, suggesting that the intrinsic activities of E protein should be displayed in the inner organelles and that plasma membrane permeabilization to monovalent ions (Pervushin et al., 2009) or to small weight compounds in E protein expressing cells (Liao et al., 2004, 2006; Madan et al., 2008), is most likely due to indirect effects. In fact, similar interpretations have been made for the increased plasma membrane permeability to small weight compounds by another viral protein with ion channel activity such as coxsackievirus 2B protein (Cornell et al., 2007; de Jong et al., 2006). This protein also locates in intracellular membranes, from where it alters protein trafficking by enhancing endocytosis processes resulting in the entry of small weight compounds. In other viral systems the intrinsic ion channel activity of specific viral proteins such as p7 protein of hepatitis C, was also restricted to intracellular membranes (Wozniak et al., 2010).

Two alternative SARS-CoV E protein topological conformations have been suggested. Studies using tagged versions of SARS-CoV E protein, suggested that this protein may have a cytosolic amino terminal domain and a carboxy terminal domain also facing the cytoplasm, or alternatively, in a minor proportion, an amino terminal cytosolic, and carboxy terminal luminal conformation, in intracellular membranes (Yuan et al., 2006). These topology models would correspond to the hairpin or to the single transmembrane pass conformations defined for SARS-CoV E protein transmembrane domain respectively (Arbely et al., 2004; Torres et al., 2006). In this work, by using highly specific antibodies for E protein amino terminal and carboxy terminal domains in selective permeabilization assays, we have clearly shown that E protein adopted an amino terminus luminal carboxy terminus cytosolic conformation in intracellular membranes of transfected and infected cells. The discrepancies on E protein amino terminus orientation with previous published data, could be due to the use of amino terminal tagged versions of E protein, which may affect the correct association of the protein with cell membranes. The model proposed here is only compatible with the single transmembrane pass described for SARS-CoV E protein, but in intracellular membranes.

Materials and methods

Viruses

The recombinant parental virus (rSARS-CoV *wt*) and a virus that lacks E gene (rSARS-CoV-ΔE) derived from the Urbani strain, were rescued from infectious cDNA clones and titrated as previously described (Almazan et al., 2006; DeDiego et al., 2007). Infections were performed in biosafety level 3 containment facilities by personnel wearing positive-pressure air-purifying respirators (HEPA AirMate; 3M, Saint Paul, MN).

Cells

The African green monkey kidney-derived Vero E6 cells were kindly provided by Eric Snijder (Medical Center, University of Leiden, The Netherlands). The human embryonic kidney-293T cells (HEK-293T) were kindly provided by Juan Ortín (CNB, Madrid, Spain).

Cells were grown at 37 °C with an atmosphere of 98% humidity, in Dulbecco's modified Eagle medium (DMEM, GIBCO) supplemented with 25 mM HEPES, 2 mM L-glutamine (SIGMA), 1% non-essential amino acids (SIGMA) and 10% fetal bovine serum (FBS, Biowhittaker).

Plasmids

The plasmid pcDNA 3.1 (+) was purchased from Invitrogen. The plasmid pcDNA-E, used to express SARS-CoV E protein, was engineered by inserting a PCR product containing the open reading frame (ORF) of SARS-CoV E gene, digested with the restriction endonucleases EcoRI and XhoI in the same sites of the pcDNA 3.1 (+) plasmid. A kozak sequence (GCCGCC) was placed immediately before the E protein ATG start codon, to improve protein translation efficiency.

Generation of monoclonal antibodies (mAbs) specific for SARS-CoV E protein

Three pairs of BALB/c mice females were respectively immunized with purified SARS-CoV E protein from one of the following sources: recombinant histidine-tagged SARS-CoV E protein, expressed using a baculovirus system; *Escherichia coli* purified E protein, obtained through the NIH Biodefense and Emerging Infections Research Resources Repository, NIAID, NIH: NR-4284; or chemically synthesized E protein, which was a gift from Jaume Torres (School of Biological Sciences, Nanyang Technological University, Singapore). Mice were immunized with three doses of 100, 50 and 50 μg of one source of protein at days 0, 21 and 35, respectively. Antigen was delivered intraperitoneally with complete Freund's adjuvant in the first immunization and with incomplete Freund's adjuvant in the following ones. Ten days after the last immunization, sera were analyzed by enzyme-linked immunosorbent assay (ELISA) using purified E protein from the three origins and by immunofluorescence using rSARS-CoV-infected Vero E6 cells. Mice that developed an antibody response to SARS-CoV E protein were selected and boosted with two consecutive doses of 40 μg of antigen. Three days later, animals were sacrificed, and spleens were collected and dissociated. Cell fusion with the murine myeloma cell line X63-Ag8.653 (Kearney et al., 1979) using the polyethylene glycol method was performed (Galfre and Milstein, 1981) and hybridomas were generated. Hybridomas were cultured in 96 multiwell plates using ClonaCell®-HY medium E (StemCell Technologies) supplemented with 10 μM azaserine. Ten days after seeding, culture supernatants were analyzed by ELISA, using the three sources of purified SARS-CoV E protein, and by immunofluorescence and Western blot, using SARS-CoV-infected cells. Hybridomas secreting specific antibodies were selected and cloned twice by limit dilution. Supernatants were analyzed 10–14 days after seeding as described above. mAbs purification from hybridoma culture supernatant was achieved by G protein affinity chromatography in HiTrap™ Protein G HP columns (GE Healthcare), and dialyzed against phosphate-buffered saline (PBS). Immunoglobulin subclass was determined by ELISA using specific antibodies against heavy chain of mouse immunoglobulins (IgG1, IgG2a, IgG2b, IgG3 and IgM) (Southern Biotech).

Generation of polyclonal antibodies (pAbs) specific for the amino terminal domain of SARS-CoV E protein

A synthetic peptide corresponding to the first 19 residues of SARS-CoV E protein (MYSFVSEETGTLIVNSVLC) was coupled to an eight branched polylysine core via a carboxy terminal cysteine to prepare multiple antigenic peptides (MAP) as described (Wilson et al., 2004). Two rabbits were immunized by Biogenes (Berlin, Germany) with 1, 0.5, 0.25 and 0.25 mg of the coupled peptide at days 1, 7, 14 and 28, respectively. Sera were collected and evaluated by ELISA, using the three sources of purified SARS-CoV E protein described above, and a peptide containing the amino terminal domain and four amino acids of the transmembrane domain of E protein (MYSFVSEETGTL). Sera were also analyzed by immunofluorescence and Western blot using pcDNA-E-transfected or SARS-CoV-infected Vero E6 cells. Rabbits producing E protein specific antibodies were boosted with 0.25 mg of coupled peptide at days 50 and 57. Final bleed sera of immunized animals were collected at day 64 and evaluated as previously described.

Confocal microscopy

Vero E6 cells were grown to 90% confluency on glass coverslips and infected with rSARS-CoV-ΔE or rSARS-CoV *wt* at a multiplicity of infection (moi) of 0.3. Alternatively, Vero E6 cells were grown to 70% confluency in 1 cm^2 wells and transfected with 1 μg of DNA using 1 μl of Lipofectamine 2000 (Invitrogen) according to the manufacturer's indications. At the indicated hours post infection (hpi) or post transfection (hpt), media were removed and cells were washed twice with PBS and fixed with 4% paraformaldehyde in PBS for 30 min at room temperature. Then, cells were washed twice with PBS and permeabilized for 10 min with 0.1% Triton X-100 in PBS. Primary antibody incubations were performed in PBS containing 10% FBS for 1 h 30 min at room temperature. Immunofluorescence was performed using mouse mAbs specific for E protein (dilution 1:5000), ERGIC53 (dilution 1:200, Alexis Biochemicals), protein disulfide isomerase (PDI, dilution 1:500, Abcam), β-tubulin (dilution 1:200, Sigma) and cadherin (dilution 1:500, Abcam). Rabbit pAbs specific for E protein (Alvarez et al., 2010), E protein amino terminal domain and PDI were used at 1:2000, 1:1000 and 1:500 dilution, respectively. Coverslips were washed four times with PBS between primary and secondary antibody incubations. Alexa 488- or Alexa 546-conjugated antibodies specific for the different species (dilution 1:500, Invitrogen) were incubated for 45 min at room temperature in PBS containing 10% FBS. Nuclei were stained using DAPI (dilution 1:200, Sigma). Coverslips were mounted in ProLong Gold anti-fade reagent (Invitrogen) and examined on a Leica SP5 confocal microscope (Leica Microsystems).

Western blot analysis

Proteins were resolved by sodium dodecyl sulfate-polyacrylamide gel electrophoresis (SDS-PAGE), transferred to a nitrocellulose membrane by wet immunotransfer and processed for Western blotting. The blots were probed using mouse mAbs specific for E protein (dilution 1:500), β-actin (dilution 1:10,000, Abcam), cadherin (dilution 1:1000, Abcam) and rabbit pAbs against E protein (dilution 1:6000) and GRP78 (1:1000, Abcam). Horseradish peroxidase-conjugated antibodies against the different species (dilution 1:40,000, Sigma) and the Immobilon Western chemiluminiscence substrate (Millipore) were used to detect bound antibodies. Chemiluminiscence was detected by exposure to Agfa X-ray film.

PEPSCAN analysis

SARS-CoV E protein sequence was represented in 34 peptides of 10 amino acids each, which overlapped in 8 amino acids with contiguous peptides. Peptides were synthesized on a cellulose membrane using the SPOT technique (Frank, 2002) at the CNB proteomics facility (Madrid, Spain). Membranes were processed as previously described for Western blot assays.

Immunoelectron microscopy

Vero E6 cells were grown to 90% confluency and infected with rSARS-CoV-ΔE or rSARS-CoV *wt* at an moi of 1. At 16 hpi, cells were fixed by adding 1 volume of fixative 2× (4% paraformaldehyde, 0.25% glutaraldehyde in sodium phosphate buffer [PB] 0.2 M pH 7.2) to the culture medium for 30 min at room temperature. Medium and fixative 2× mixture were replaced by a fixative 1× solution (2% paraformaldehyde, 0.125% glutaraldehyde in PB 0.1 M pH 7.2), and incubated for 1 h 30 min at 4 °C. Fixative was removed, and cells were scrapped and pelleted. After washing with PB containing 50 mM glycine, cells were embedded in 12% gelatine and infused in 2.3 M sucrose. Mounted gelatine blocks were frozen in liquid nitrogen. Thin sections were prepared in an ultracryomicrotome (Leica EM Ultracut UC6/FC6, Vienna, Austria). Ultrathin cryosections were collected with 2% methylcellulose in 2.3 M sucrose. Cryosections were incubated at room temperature on drops of 2% gelatin in PBS for 20 min at 37 °C, followed by 50 mM glycine in PBS during 15 min, 10% FBS in PBS during 10 min and 5% FBS in PBS 5 min. Then, cryosections were incubated with SARS-CoV E protein specific mAb E5 (dilution 1:250) in PBS containing 5% FBS for 30 min at room temperature. After three washes with drops of PBS for 10 min, sections were incubated for 20 min using mouse IgG specific antibody coupled to 10 nm diameter colloidal gold particles using a 1:100 dilution in 5% FBS/PBS. Cryosections were washed three times with drops of PBS for 10 min and twice with distilled water. As a control for non-specific binding of the colloidal gold-conjugated antibody, the primary antibody was omitted. Cells were observed using a Jeol Electron Microscope (JEM 1020) with a CCD camera SIS Megaview III.

Plasma membrane protein biotinylation

Vero E6 cells were grown to 70% confluency in 75 cm^2 flasks and either mock transfected, or transfected with 37.5 μg of empty pcDNA 3.1 (+) or pcDNA-E plasmids using 37.5 μl of Lipofectamine 2000 (Invitrogen) according to manufacturer's instructions. In parallel, Vero E6 cells were grown to 90% confluency and infected with rSARS-CoV-ΔE or rSARS-CoV *wt* at an moi of 0.3. At 24 hpt or hpi, cell surface proteins were biotin labeled using the Cell Surface Protein Isolation Kit (Pierce) following the manufacturer's indications. Briefly, cells were rinsed twice with ice-cold PBS, and incubated with EZ-link Sulfo-NHS-SS-biotin for 15 min at 4 °C to biotinylate surface proteins. Reaction was quenched, cells were washed twice with PBS and scrapped. Cells were pelleted, lysed and cell extracts were clarified by centrifugation. Biotin labeled proteins were purified using affinity chromatography, by incubating cell extracts for 1 h with a neutravidin Sepharose resin. Resin was washed three times, and bound proteins were eluted by adding SDS-sample buffer.

Whole-cell patch clamp

HEK-293T cells were grown to 70% confluency in 12.5 cm^2 flasks and transfected with 12.5 μg of DNA using 37.5 μl of Lipofectamine 2000 (Invitrogen) according to manufacturer's indications. At 8 hpt cells were trypsinized and seeded onto poly-L-lysine coated glass coverslips. At 24 hpt whole-cell currents were recorded at room temperature using an Axopatch 1D amplifier (Axon instruments). Cells were placed in a bath solution containing (in mM): 5 KCl, 135 NaCl, 1 $MgCl_2$, 2 $CaCl_2$, 10 Glucose, 10 HEPES, and BSA 0.001% pH 7.4 and filled through the electrode with a solution containing (in mM): 110 KCl, 5 NaCl, 0.5 $CaCl_2$, 5 EGTA, 2 $MgCl_2$ and 10 HEPES pH 7.2. The voltage clamp protocol consisted of rectangular voltage steps of 40 ms

duration from −160 mV to +140 mV in 20 mV increments applied from a holding potential of −40 mV.

Pull-down assays

Vero E6 cells were grown to 90% confluence and mock infected, infected at an moi of 0.1 with rSARS-CoV *wt* or with a virus containing a tagged E protein (rSARS-CoV-ETagCt) for further purification of associated protein complexes (Alvarez et al., 2010). Cell extracts, tandem affinity purification and mass spectrometry were performed as previously described to identify SARS-CoV E bound proteins (Alvarez et al., 2010).

Plasma membrane selective permeabilization assays

Prior to fixation, cells were placed on ice and rinsed twice with KHM buffer (110 mM potassium acetate, 2 mM magnesium acetate, and 20 mM HEPES pH 7.2). After that, the plasma membrane of cells was selectively permeabilized with 25 μg/ml of digitonin (Sigma) in KHM buffer for 5 min at 4 °C. Then, cells were washed twice with KHM buffer, fixed with 4% paraformaldehyde in PBS for 30 min at room temperature and subjected to immunofluorescence as described before.

Acknowledgments

This work was supported by grants from the Ministry of Science and Innovation of Spain (BIO2007-60978 and BIO2010-16705), the European Community's Seventh Framework Programme (FP7/2007–2013) under the project "EMPERIE" EC Grant Agreement number 223498, U.S. National Institutes of Health (ARRA-W000151845) and Consejo Superior de Investigaciones Cientificas (CSIC) of Spain (CSIC-200920I016 and CSIC-201120E007). JLN received a fellowship from CSIC. We thank Monica Garcia-Gallo and Laura Martin for help in monoclonal antibody production and purification (Protein tools, CNB), Fernando Roncal (CNB, Proteomics facility) for his advice on PEPSCAN assays, Cristina Patiño and Javier Bueno for advise in immunoelectron microscopy assays (CNB, Electron Microscopy facility), Pedro de la Villa, Javier Vicente and Laura Ramirez (Physiology department, UAH, Madrid) for help in patch-clamp assays, Jaume Torres for provide reagents, Alberto Perez (Physiology department, UAM, Madrid) for the discussion of the manuscript and Marga Gonzalez for her technical assistance.

References

Almazan, F., DeDiego, M.L., Galan, C., Escors, D., Alvarez, E., Ortego, J., Sola, I., Zuñiga, S., Alonso, S., Moreno, J.L., Nogales, A., Capiscol, C., Enjuanes, L., 2006. Construction of a SARS-CoV infectious cDNA clone and a replicon to study coronavirus RNA synthesis. J. Virol. 80, 10900–10906.

Alvarez, E., DeDiego, M.L., Nieto-Torres, J.L., Jimenez-Guardeno, J.M., Marcos-Villar, L., Enjuanes, L., 2010. The envelope protein of severe acute respiratory syndrome coronavirus interacts with the non-structural protein 3 and is ubiquitinated. Virology 402, 281–291.

Arbely, E., Khattari, Z., Brotons, G., Akkawi, M., Salditt, T., Arkin, I.T., 2004. A highly unusual palindromic transmembrane helical hairpin formed by SARS coronavirus E protein. J. Mol. Biol. 341, 769–779.

Chu, D.K., Peiris, J.S., Chen, H., Guan, Y., Poon, L.L., 2008. Genomic characterizations of bat coronaviruses (1A, 1B and HKU8) and evidence for co-infections in Miniopterus bats. J. Gen. Virol. 89, 1282–1287.

Cornell, C.T., Kiosses, W.B., Harkins, S., Whitton, J.L., 2007. Coxsackievirus B3 proteins directionally complement each other to downregulate surface major histocompatibility complex class I. J. Virol. 81, 6785–6797.

Corse, E., Machamer, C.E., 2000. Infectious bronchitis virus E protein is targeted to the Golgi complex and directs release of virus-like particles. J. Virol. 74, 4319–4326.

de Haan, C.A.M., Smeets, M., Vernooij, F., Vennema, H., Pottier, P.J.M., 1999. Mapping of the coronavirus membrane protein domains involved in interaction with the spike protein. J. Virol. 73, 7441–7452.

de Jong, A.S., Visch, H.J., de Mattia, F., van Dommelen, M.M., Swarts, H.G., Luyten, T., Callewaert, G., Melchers, W.J., Willems, P.H., van Kuppeveld, F.J., 2006. The coxsackievirus 2B protein increases efflux of ions from the endoplasmic reticulum and Golgi, thereby inhibiting protein trafficking through the Golgi. J. Biol. Chem. 281, 14144–14150.

DeDiego, M.L., Alvarez, E., Almazan, F., Rejas, M.T., Lamirande, E., Roberts, A., Shieh, W.J., Zaki, S.R., Subbarao, K., Enjuanes, L., 2007. A severe acute respiratory syndrome coronavirus that lacks the E gene is attenuated in vitro and in vivo. J. Virol. 81, 1701–1713.

DeDiego, M.L., Pewe, L., Alvarez, E., Rejas, M.T., Perlman, S., Enjuanes, L., 2008. Pathogenicity of severe acute respiratory coronavirus deletion mutants in hACE-2 transgenic mice. Virology 376, 379–389.

Drexler, J.F., Gloza-Rausch, F., Glende, J., Corman, V.M., Muth, D., Goettsche, M., Seebens, A., Niedrig, M., Pfefferle, S., Yordanov, S., Zhelyazkov, L., Hermanns, U., Vallo, P., Lukashev, A., Muller, M.A., Deng, H., Herrler, G., Drosten, C., 2010. Genomic characterization of severe acute respiratory syndrome-related coronavirus in European bats and classification of coronaviruses based on partial RNA-dependent RNA polymerase gene sequences. J. Virol. 84, 11336–11349.

Drosten, C., Gunther, S., Preiser, W., van der Werf, S., Brodt, H.R., Becker, S., Rabenau, H., Panning, M., Kolesnikova, L., Fouchier, R.A., Berger, A., Burguiere, A.M., Cinatl, J., Eickmann, M., Escriou, N., Grywna, K., Kramme, S., Manuguerra, J.C., Muller, S., Rickerts, V., Sturmer, M., Vieth, S., Klenk, H.D., Osterhaus, A.D., Schmitz, H., Doerr, H.W., 2003. Identification of a novel coronavirus in patients with severe acute respiratory syndrome. N. Engl. J. Med. 348, 1967–1976.

Enjuanes, L., Almazan, F., Sola, I., Zuniga, S., 2006. Biochemical aspects of coronavirus replication and virus–host interaction. Annu. Rev. Microbiol. 60, 211–230.

Enjuanes, L., Gorbalenya, A.E., de Groot, R.J., Cowley, J.A., Ziebuhr, J., Snijder, E.J., 2008. The Nidovirales, Third Edition. In: Mahy, B.W.J., Van Regenmortel, M., Walker, P., Majumder-Russell, D. (Eds.), Encyclopedia of Virology, 5 vols.. Elsevier Ltd., Oxford, pp. 419–430.

Ewart, G.D., Sutherland, T., Gage, P.W., Cox, G.B., 1996. The Vpu protein of human immunodeficiency virus type 1 forms cation-selective ion channels. J. Virol. 70, 7108–7115.

Frank, R., 2002. The SPOT-synthesis technique. Synthetic peptide arrays on membrane supports—principles and applications. J. Immunol. Methods 267, 13–26.

Galfre, G., Milstein, C., 1981. Preparation of monoclonal antibodies: strategies and procedures. In: Langone, J.J., Van Vunakis, H. (Eds.), Immunochemical Techniques, Vol. 73. Academic Press, New York, pp. 3–46.

Godet, M., L'Haridon, R., Vautherot, J.F., Laude, H., 1992. TGEV coronavirus ORF4 encodes a membrane protein that is incorporated into virions. Virology 188, 666–675.

Gosert, R., Kanjanahaluethai, A., Egger, D., Bienz, K., Baker, S.C., 2002. RNA replication of mouse hepatitis virus takes place at double-membrane vesicles. J. Virol. 76, 3697–3708.

Huang, C., Ito, N., Tseng, C.T., Makino, S., 2006. Severe acute respiratory syndrome coronavirus 7a accessory protein is a viral structural protein. J. Virol. 80, 7287–7294.

Huang, C., Peters, C.J., Makino, S., 2007. Severe acute respiratory syndrome coronavirus accessory protein 6 is a virion-associated protein and is released from 6 protein-expressing cells. J. Virol. 81, 5423–5426.

Ji, H.L., Song, W., Gao, Z., Su, X.F., Nie, H.G., Jiang, Y., Peng, J.B., He, Y.X., Liao, Y., Zhou, Y.J., Tousson, A., Matalon, S., 2009. SARS-CoV proteins decrease levels and activity of human ENaC via activation of distinct PKC isoforms. Am. J. Physiol. Lung Cell. Mol. Physiol. 296, L372–L383.

Kaplan, J.H., 2002. Biochemistry of Na,K-ATPase. Annu. Rev. Biochem. 71, 511–535.

Kearney, J.F., Radbruch, A., Liesegang, B., Rajewsky, K., 1979. A new mouse myeloma cell line that has lost immunoglobulin expression but permits the construction of antibody-secreting hybrid cell lines. J. Immunol. 123, 1548–1550.

Kuo, L., Masters, P.S., 2003. The small envelope protein E is not essential for murine coronavirus replication. J. Virol. 77, 4597–4608.

Li, W., Moore, M.J., Vasilieva, N., Sui, J., Wong, S.K., Berne, M.A., Somasundaran, M., Sullivan, J.L., Luzuriaga, K., Greenough, T.C., Choe, H., Farzan, M., 2003. Angiotensin-converting enzyme 2 is a functional receptor for de SARS coronavirus. Nature 426, 450–454.

Liao, Y., Lescar, J., Tam, J.P., Liu, D.X., 2004. Expression of SARS-coronavirus envelope protein in *Escherichia coli* cells alters membrane permeability. Biochem. Biophys. Res. Commun. 325, 374–380.

Liao, Y., Yuan, Q., Torres, J., Tam, J.P., Liu, D.X., 2006. Biochemical and functional characterization of the membrane association and membrane permeabilizing activity of the severe acute respiratory syndrome coronavirus envelope protein. Virology 349, 264–265.

Lim, K.P., Liu, D.X., 2001. The missing link in coronavirus assembly. Retention of the avian coronavirus infectious bronchitis virus envelope protein in the pre-Golgi compartments and physical interaction between the envelope and membrane proteins. J. Biol. Chem. 276, 17515–17523.

Madan, V., Castello, A., Carrasco, L., 2008. Viroporins from RNA viruses induce caspase-dependent apoptosis. Cell. Microbiol. 10 (2), 437–451.

Maeda, J., Repass, J.F., Maeda, A., Makino, S., 2001. Membrane topology of coronavirus E protein. Virology 281, 163–169.

Masters, P.S., 2006. The molecular biology of coronaviruses. Adv. Virus Res. 66, 193–292.

Muller, M.A., Paweska, J.T., Leman, P.A., Drosten, C., Grywna, K., Kemp, A., Braack, L., Sonnenberg, K., Niedrig, M., Swanepoel, R., 2007. Coronavirus antibodies in African bat species. Emerg. Infect. Dis. 13, 1367–1370.

Nal, B., Chan, C., Kien, F., Siu, L., Tse, J., Chu, K., Kam, J., Staropoli, I., Crescenzo-Chaigne, B., Escriou, N., van der Werf, S., Yuen, K.Y., Altmeyer, R., 2005. Differential maturation and subcellular localization of severe acute respiratory syndrome coronavirus surface proteins S, M and E. J. Gen. Virol. 86, 1423–1434.

Narayanan, K., Maeda, A., Maeda, J., Makino, S., 2000. Characterization of the coronavirus M protein and nucleocapsid interaction in infected cells. J. Virol. 74, 8127–8134.

Netland, J., DeDiego, M.L., Zhao, J., Fett, C., Alvarez, E., Nieto-Torres, J.L., Enjuanes, L., Perlman, S., 2010. Immunization with an attenuated severe acute respiratory syndrome coronavirus deleted in E protein protects against lethal respiratory disease. Virology 399, 120–128.

Nguyen, V.-P., Hogue, B.G., 1997. Protein interactions during coronavirus assembly. J. Virol. 71, 9278–9284.

Ortego, J., Escors, D., Laude, H., Enjuanes, L., 2002. Generation of a replication-competent, propagation-deficient virus vector based on the transmissible gastroenteritis coronavirus genome. J. Virol. 76, 11518–11529.

Ortego, J., Ceriani, J.E., Patino, C., Plana, J., Enjuanes, L., 2007. Absence of E protein arrests transmissible gastroenteritis coronavirus maturation in the secretory pathway. Virology 368, 296–308.

Pervushin, K., Tan, E., Parthasarathy, K., Lin, X., Jiang, F.L., Yu, D., Vararattanavech, A., Soong, T.W., Liu, D.X., Torres, J., 2009. Structure and inhibition of the SARS coronavirus envelope protein ion channel. PLoS Pathog. 5, e1000511.

Pinto, L.H., Holsinger, L.J., Lamb, R.A., 1992. Influenza virus M2 protein has ion channel activity. Cell 69, 517–528.

Price, M.P., Thompson, R.J., Eshcol, J.O., Wemmie, J.A., Benson, C.J., 2004. Stomatin modulates gating of acid-sensing ion channels. J. Biol. Chem. 279, 53886–53891.

Quan, P.L., Firth, C., Street, C., Henriquez, J.A., Petrosov, A., Tashmukhamedova, A., Hutchison, S.K., Egholm, M., Osinubi, M.O., Niezgoda, M., Ogunkoya, A.B., Briese, T., Rupprecht, C.E., Lipkin, W.I., 2010. Identification of a severe acute respiratory syndrome coronavirus-like virus in a leaf-nosed bat in Nigeria. MBio 1, e00208–e00210.

Raamsman, M.J.B., Locker, J.K., de Hooge, A., de Vries, A.A.F., Griffiths, G., Vennema, H., Rottier, P.J.M., 2000. Characterization of the coronavirus mouse hepatitis virus strain A59 small membrane protein E. J. Virol. 74, 2333–2342.

Rota, P.A., Oberste, M.S., Monroe, S.S., Nix, W.A., Campganoli, R., Icenogle, J.P., Peñaranda, S., Bankamp, B., Maher, K., Chen, M.-H., Tong, S., Tamin, A., Lowe, L., Frace, M., DeRisi, J.L., Chen, Q., Wang, D., Erdman, D.D., Peret, T.C.T., Burns, C., Ksiazek, T.G., Rollin, P.E., Sanchez, A., Liffick, S., Holloway, B., Limor, J., McCaustland, K., Olsen-Rassmussen, M., Fouchier, R., Gunther, S., Osterhaus, A.D.M.E., Drosten, C., Pallansch, M.A., Anderson, L.J., Bellini, W.J., 2003. Characterization of a novel coronavirus associated with severe acute respiratory syndrome. Science 300, 1394–1399.

Sawicki, S.G., Sawicki, D.L., 1990. Coronavirus transcription: subgenomic mouse hepatitis virus replicative intermediates function in RNA synthesis. J. Virol. 64, 1050–1056.

Schaecher, S.R., Mackenzie, J.M., Pekosz, A., 2007. The ORF7b protein of SARS-CoV is expressed in virus-infected cells and incorporated into SARS-CoV particles. J. Virol. 81, 718–731.

Shen, S., Lin, P.S., Chao, Y.C., Zhang, A., Yang, X., Lim, S.G., Hong, W., Tan, Y.J., 2005. The severe acute respiratory syndrome coronavirus 3a is a novel structural protein. Biochem. Biophys. Res. Commun. 330, 286–292.

Snijder, E.J., van der Meer, Y., Zevenhoven-Dobbe, J., Onderwater, J.J., van der Meulen, J., Koerten, H.K., Mommaas, A.M., 2006. Ultrastructure and origin of membrane vesicles associated with the severe acute respiratory syndrome coronavirus replication complex. J. Virol. 80, 5927–5940.

Tooze, J., Tooze, S.A., Fuller, S.D., 1987. Sorting of progeny coronavirus from condensed secretory proteins at the exit from the trans-golgi network of atT20 cells. J. Cell Biol. 105, 1215–1226.

Torres, J., Parthasarathy, K., Lin, X., Saravanan, R., Liu, D.X., 2006. Model of a putative pore: the pentameric alpha-helical bundle of SARS coronavirus E protein in lipid bilayers. Biophys. J. 91, 938–947.

Torres, J., Maheswari, U., Parthasarathy, K., Ng, L., Liu, D.X., Gong, X., 2007. Conductance and amantadine binding of a pore formed by a lysine-flanked transmembrane domain of SARS coronavirus envelope protein. Protein Sci. 16, 2065–2071.

van der Hoek, L., Pyrc, K., Jebbink, M.F., Vermeulen-Oost, W., Berkhout, R.J., Wolthers, K.C., Wertheim-van Dillen, P.M., Kaandorp, J., Spaargaren, J., Berkhout, B., 2004. Identification of a new human coronavirus. Nat. Med. 10, 368–373.

van der Most, R.G., Spaan, W.J.M., 1995. Coronavirus replication, transcription, and RNA recombination. In: Siddell, S.G. (Ed.), The Coronaviridae. Plenum Press, New York, pp. 11–31.

Weiss, S.R., Navas-Martin, S., 2005. Coronavirus pathogenesis and the emerging pathogen severe acute respiratory syndrome coronavirus. Microbiol. Mol. Biol. Rev. 69, 635–664.

Wilson, L., McKinlay, C., Gage, P., 2004. SARS coronavirus E protein forms cation-selective ion channels. Virology 330, 322–331.

Wilson, L., Gage, P., Ewart, G., 2006. Hexamethylene amiloride blocks E protein ion channels and inhibits coronavirus replication. Virology 353, 294–306.

Wong, S.K., Li, W., Moore, M.J., Choe, H., Farzan, M., 2004. A 193-amino acid fragment of the SARS coronavirus S protein efficiently binds angiotensin-converting enzyme 2. J. Biol. Chem. 279, 3197–3201.

Wozniak, A.L., Griffin, S., Rowlands, D., Harris, M., Yi, M., Lemon, S.M., Weinman, S.A., 2010. Intracellular proton conductance of the hepatitis C virus p7 protein and its contribution to infectious virus production. PLoS Pathog. 6, e1001087.

Yuan, Q., Liao, Y., Torres, J., Tam, J.P., Liu, D.X., 2006. Biochemical evidence for the presence of mixed membrane topologies of the severe acute respiratory syndrome coronavirus envelope protein expressed in mammalian cells. FEBS Lett. 580, 3192–3200.

Ziebuhr, J., 2005. The coronavirus replicase. In: Enjuanes, L. (Ed.), Coronavirus Replication and Reverse Genetics, Vol. 287. Springer, pp. 57–94.

Ziebuhr, J., Snijder, E.J., Gorbalenya, A.E., 2000. Virus-encoded proteinases and proteolytic processing in the *Nidovirales*. J. Gen. Virol. 81, 853–879.

Zuñiga, S., Cruz, J.L., Sola, I., Mateos-Gomez, P.A., Palacio, L., Enjuanes, L., 2010. Coronavirus nucleocapsid protein facilitates template switching and is required for efficient transcription. J. Virol. 84, 2169–2175.